

## Fructose-1,6-bisphosphatase: Arginine-22 Is Involved in Stabilization of the T Allosteric State<sup>†</sup>

Guqiang Lu, Mark K. Williams, Eugene L. Giroux, and Evan R. Kantrowitz\*

Department of Chemistry, Merkert Chemistry Center, Boston College, Chestnut Hill, Massachusetts 02167

Received June 21, 1995; Revised Manuscript Received August 14, 1995<sup>®</sup>

**ABSTRACT:** A comparison of the X-ray crystallographic structures of the R and T allosteric states [Ke, H. M., Liang, J.-Y., Zhang, Y., & Lipscomb, W. N. (1991) *Biochemistry* 30, 4412–4420] of the pig kidney fructose-1,6-bisphosphatase (EC 3.1.3.11) reveals major changes in the quaternary structure of the enzyme upon the binding of the allosteric inhibitor AMP. This change in quaternary structure involves the breaking of one set of interactions that stabilize the R state and the formation of another set of interactions that stabilize the T state of the enzyme. In particular, the interactions of Arg-22 with nearby amino acid residues are quite different in the R and T states of the enzyme. Although the crystallographic data suggest that intersubunit interactions such as those involving Arg-22 are important for stabilization of the R and/or T states, the X-ray structures do not provide direct evidence concerning the functional role of specific amino acid residues. Therefore, site-specific mutagenesis has been used to probe the function of Arg-22 in pig kidney fructose-1,6-bisphosphatase. The replacement of Arg-22 by Ala results in a mutant enzyme with enhanced catalytic efficiency compared to the wild-type, as indicated by a kinetic analysis showing a slightly lower  $K_m$  and increased  $V_{max}$  compared to the wild-type enzyme. In addition, the substitution enhances both substrate inhibition and the affinity of the inhibitor fructose 2,6-bisphosphate. Moreover, the replacement of Arg-22 by Ala results in a more than 10-fold loss of the ability of AMP to inhibit the enzyme. These results are consistent with a role of Arg-22 in the preferential stabilization of the noncatalytic T state of the enzyme.

Fructose-1,6-bisphosphatase (EC 3.1.3.11) catalyzes the hydrolysis of fructose 1,6-bisphosphate (Fru-1,6- $P_2$ )<sup>1</sup> to fructose 6-phosphate and inorganic phosphate ( $P_i$ ) in the gluconeogenesis pathway and plays a key role in regulation of this pathway. The physiological regulators AMP and fructose 2,6-bisphosphate negatively modulate Fru-1,6- $P_2$ -ase activity and, in reciprocal fashion, positively affect the activity of phosphofructokinase, a control point in glycolysis [for a recent review, see Pilkis and Claus (1991)]. Fru-1,6- $P_2$ ases are multimeric enzymes consisting of four identical subunits. Each subunit of the pig kidney enzyme consists of 337 amino acid residues corresponding to a molecular weight of about 36 500 (Marcus et al., 1982; Williams & Kantrowitz, 1992).

Hydrolysis of substrate by Fru-1,6- $P_2$ ase displays hyperbolic kinetics at neutral pH, with partial inhibition at high substrate concentrations, whereas plots of reaction velocity versus concentration of the cofactor magnesium are sigmoidal (Nimmo & Tipton, 1975b). Inhibition by AMP is cooperative, with a Hill coefficient near 2 (Nimmo & Tipton, 1975a; Taketa & Pogell, 1965) while Fru-2,6- $P_2$  binds to the active

sites of the enzyme (Ke et al., 1989a) in competition with the substrate Fru-1,6- $P_2$  (Pilkis et al., 1981).

Investigations of the catalytic and regulatory mechanisms of Fru-1,6- $P_2$ ase have been enhanced by the availability of crystal structures for pig kidney Fru-1,6- $P_2$ ase (Ke et al., 1989b) and complexes of this enzyme with the hydrolytic product fructose 6-phosphate (Ke et al., 1991b), with the inhibitor AMP (Ke et al., 1991a), and with the inhibitor Fru-2,6- $P_2$  (Ke et al., 1989a), among others [for a recent review, see Liang et al. (1992)]. The tertiary structure of each subunit is divided into two folding domains, the AMP and the Fru-1,6- $P_2$  domains (Liang et al., 1992). The AMP binding site in each subunit is approximately 30 Å distant from the active site (Ke et al., 1991a), and metal binding sites are located between the Fru-1,6- $P_2$  and AMP domains (Ke et al., 1990).

On the basis of the crystal structures of the R (Ke et al., 1991b) and the T (Ke et al., 1991a) allosteric states, Lipscomb and co-workers (Zhang et al., 1994) have proposed structural details concerning the allosteric transition in pig kidney Fru-1,6- $P_2$ ase. The R → T transition of pig kidney Fru-1,6- $P_2$ ase involves a 17° rotation of the C1:C2<sup>2</sup> dimer with respect to the C3:C4 dimer. This rotation dramatically alters the interactions across the C1:C4 interface (as well as

<sup>†</sup> Supported by Grant MCB-9303798 from the National Science Foundation.

\* To whom correspondence should be addressed.

<sup>®</sup> Abstract published in *Advance ACS Abstracts*, October 1, 1995.

<sup>1</sup> Abbreviations: Fru-1,6- $P_2$ ase, fructose-1,6-bisphosphatase; Fru-1,6- $P_2$ , fructose 1,6-bisphosphate; Fru-2,6- $P_2$ , fructose 2,6-bisphosphate; Arg-22 → Ala, mutant pig kidney fructose-1,6-bisphosphatase with alanine in place of arginine at position 22.

<sup>2</sup> The four subunits of fructose-1,6-bisphosphatase are designated C1, C2, C3, and C4 and labeled clockwise. The C1 and C2 subunits correspond to the upper dimer, and the C3 and C4 subunits correspond to the lower dimer. Therefore, C4 is below C1 and C3 is below C2 [for additional details, see Ke et al. (1991a)].

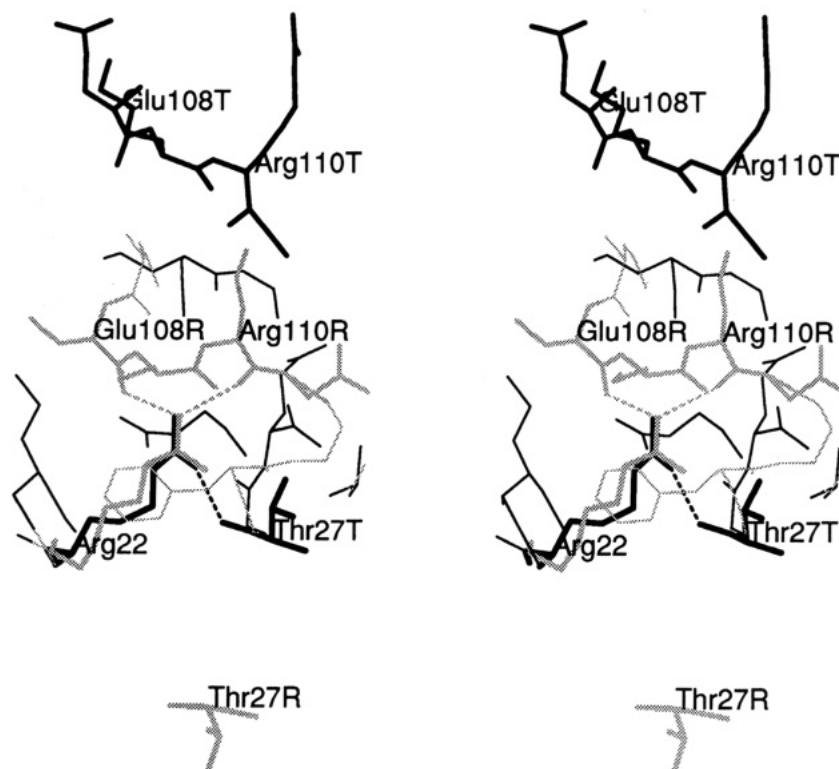


FIGURE 1: Stereoview of the C2:C3 interface region of Fru-1,6- $P_2$ ase in the R (gray) and T (black) allosteric states near Arg-22. In the T state, Arg-22 (C3) interacts with Thr-27 (C2), while in the R state, Arg-22 (C3) interacts with the backbone carbonyls of Glu-108 (C2) and Arg-110 (C2).

the symmetry-related C2:C3 interface). For example, in the R state, both Glu-108 and Arg-110 interact with Arg-22<sup>3</sup> (Ke et al., 1991b), while in the T state Arg-22 interacts with Thr-27 and Glu-29<sup>4</sup> (Ke et al., 1991a) as illustrated in Figure 1. The AMP binding site is located close to this area of the structure, and Lipscomb and co-workers have proposed that the mechanism of allosteric regulation may be critically related to a number of residues in the AMP binding site including Thr-27, which interacts with Arg-22 in the T state (Ke et al., 1991a). In order to determine whether the interactions involving Arg-22 are critical for the stabilization of either the T or the R states of fructose 1,6-phosphatase and to evaluate the importance of the C1:C4 and the C2:C3 interfaces for allosteric regulation, we have used site-specific mutagenesis to replace Arg-22 with alanine in the cloned pig kidney enzyme (Williams & Kantrowitz, 1992). The mutant enzyme (Arg-22  $\rightarrow$  Ala) was expressed in *E. coli*, and consequences of this mutation on the kinetic properties of Fru-1,6- $P_2$ ase were examined.

## EXPERIMENTAL PROCEDURES

**Materials.** Agar, agarose, ampicillin, chloramphenicol, sodium dihydrogen phosphate, and magnesium chloride were purchased from Sigma Chemical Co. Tris and enzyme-grade ammonium sulfate were supplied by ICN Biomedicals. Tryptone and yeast extract were from Difco Laboratories. All the reagents needed for DNA sequencing were obtained from U.S. Biochemical. Restriction endonucleases, T4 DNA ligase, T4 DNA polymerase, and T4 polynucleotide kinase were either from U.S. Biochemical or New England Biolabs, and used according to the supplier's recommendations. DNA

fragments were isolated from agarose gels with the GeneClean II kit from Bio 101 Inc.

**Strains.** The *E. coli* K12 strain MV1190 [ $\Delta(lac-proAB)$ , *supE*, *thi*,  $\Delta(sri-recA)$  306::Tn10(*tet*<sup>r</sup>)/F' *traD36*, *proAB*, *lacI<sup>q</sup>*, *lacZ* $\Delta$ M15], phagemid pUC119, and the M13 phage M13K07 were obtained from J. Messing. The strain CJ236 [*dut-1*, *ung-1*, *thi-1*, *relA-1*/pCJ105(Cm<sup>r</sup>)] was a gift of T. Kunkel, while EK1601 [*tonA22*,  $\lambda$ DE3, *ompF*627(T<sub>2</sub><sup>R</sup>), *relA1*, *pit-10*, *spoT1*,  $\Delta(fbp)$ 287], a derivative of DF657 (Sedivy et al., 1984), was constructed in this laboratory (Giroux et al., 1994). *E. coli* strain XL1-Blue MRF<sup>+</sup> [ $\Delta(mcrA)$ 183,  $\Delta(mcrCB-hsdSMR-mrr)$ 172, *endA1*, *supE44*, *thi-1*, *recA*, *gyrA96*, *relA1*, *lac*,  $\lambda^-$ /F' *proAB*, *lacI<sup>q</sup>*, *lacZ* $\Delta$ M15, Tn10(*tet*<sup>r</sup>)] was from Stragene (La Jolla, CA).

**Methods. Oligonucleotide Synthesis.** The oligonucleotides required for site-specific mutagenesis and the sequencing primers were synthesized on an Applied Biosystems 381A DNA synthesizer and purified by HPLC employing a DuPont Zorbay Oligo ion-exchange column.

**Construction of the Arg-22  $\rightarrow$  Ala Mutation.** Complementary DNA for pig kidney Fru-1,6- $P_2$ ase was previously cloned from a 1.3 kb *Bst*XI fragment inserted into the vector pcDNA II (Williams & Kantrowitz, 1992). A *Hind*III-*Xba*I fragment was excised from this plasmid and cloned into the vector pUC119 to give phagemid pEK178. Sequencing of mutations in pEK178 was simplified because it contained the M13 intergenic region, allowing isolation of single-stranded DNA after coinfection with a helper phage.

Site-specific mutagenesis was performed on the cDNA of Fru-1,6- $P_2$ ase harbored on plasmid pEK178, employing the method of Kunkel (1985, 1987). Uracil-containing single-stranded DNA was obtained by infection of *E. coli* strain CJ236 containing pEK178 with helper phage M13K07 (Vieira & Messing, 1987). Two primers were used simul-

<sup>3</sup> This interaction is only observed in the C2:C3 interface.

<sup>4</sup> This interaction is only observed in the C1:C4 interface.

taneously to introduce both the Arg-22 → Ala mutation as well as an *NdeI* restriction site at the translational start of the cDNA of the Fru-1,6-*P*<sub>2</sub>ase gene. The introduction of the *NdeI* site did not alter the amino acid sequence of the Fru-1,6-*P*<sub>2</sub>ase. Potential mutant candidates were initially screened by restriction analysis of double-stranded DNA to determine whether the *NdeI* site had been introduced. Those candidates containing the new *NdeI* restriction site were further screened by DNA sequence analysis (Sanger et al., 1977). Both the introduction of the *NdeI* site at the translation start and the Arg-22 → Ala mutation were confirmed in this fashion. The resultant plasmid, pEK212, contained both the Arg-22 → Ala mutation as well as the *NdeI* site at the translational start site.

**Construction of Expression Phagemid for the Arg-22 → Ala Fru-1,6-*P*<sub>2</sub>ase.** In order to express the Arg-22 → Ala Fru-1,6-*P*<sub>2</sub>ase, the phagemids pEK212 and pET23a (Novagen, Inc.) were first treated with the restriction enzymes *NotI* and *BamHI*. The fragment from pEK212 coding for the mutant Fru-1,6-*P*<sub>2</sub>ase and the large fragment of pET23a, containing most of the vector, were mixed and treated with T4 DNA ligase. After transformation into XL1-Blue MRF<sup>+</sup>, an intermediate construct was isolated and cleaved with *NdeI* to remove a small *NdeI*–*NdeI* fragment. The larger fragment was isolated and then circularized by treatment with T4 DNA ligase. Likely candidates, identified by restriction analysis, were confirmed by DNA sequence analysis (Sanger et al., 1977) in order to verify the presence of both the Arg-22 → Ala mutation and the *NdeI* site at the translational start of the Fru-1,6-*P*<sub>2</sub>ase gene. The final phagemid was identified as pEK279.

**Expression of Pig Kidney Fru-1,6-*P*<sub>2</sub>ase in *E. coli*.** In order to express the wild-type and Arg-22 → Ala pig kidney Fru-1,6-*P*<sub>2</sub>ases, phagemids pEK188 and pEK279, respectively, were transformed into *E. coli* strain EK1601. *E. coli* strain EK1601 has a deletion in the chromosomal *fbp* gene and can be induced to produce T7 RNA polymerase (Giroux et al., 1994). Therefore, it was impossible to contaminate the pig kidney Fru-1,6-*P*<sub>2</sub>ase expressed from the plasmid with *E. coli* Fru-1,6-*P*<sub>2</sub>ase expressed from the chromosome.

**Enzyme Purification.** Bacteria were cultured with vigorous agitation at 37 °C in M9 medium supplemented with 0.5% casamino acids and ampicillin at 100 µg/mL. Induction of T7 RNA polymerase was initiated by addition of 0.4 mM isopropyl β-D-thiogalactopyranoside (U.S. Biochemical). After further cultivation for 16–22 h, cells were harvested by centrifugation, and then broken open by a freeze–thaw procedure (El-Maghrabi & Pilkis, 1991). The purification of the Arg-22 → Ala enzyme was accomplished by the method previously described (Giroux et al., 1994).

**Fru-1,6-*P*<sub>2</sub>ase Assays and Data Analysis.** A spectrophotometric, coupled enzyme assay was employed to measure Fru-1,6-*P*<sub>2</sub>ase activity (Riou et al., 1977). Standard conditions (2 mM magnesium chloride, 17.5 µM Fru-1,6-*P*<sub>2</sub>) were used to determine specific activity. Digital absorbance values were collected over a 6 min assay interval and fit to a straight line by computer, using data beyond the coupling lag period. In all assays, the substrate Fru-1,6-*P*<sub>2</sub> was added last, after incubation and thermal equilibration of enzyme, magnesium (and inhibitor) components. One unit of enzyme activity causes reduction of 1 µmol of NADP per minute at 30 °C.

Methods used to determine the kinetic model parameters were described previously (Giroux et al., 1994). Substrate

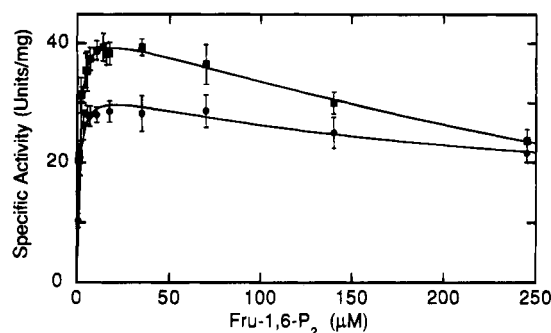


FIGURE 2: Dependence of the activity of wild-type (●) and the Arg-22 → Ala (■) Fru-1,6-*P*<sub>2</sub>ases on the concentration of Fru-1,6-*P*<sub>2</sub> at 2 mM Mg<sup>2+</sup>. Assays were performed in Tris buffer, pH 7.5, at 30 °C. All data points are the average of at least 4 determinations. The error bars indicate plus and minus one standard deviation, and the curves drawn are the best-fit curves calculated by a nonlinear least-squares procedure to the Michaelis–Menten equation incorporating a term for substrate inhibition.

saturation curves for both the wild-type and mutant enzymes were fit by nonlinear regression to a modified form of the Michaelis–Menten equation which incorporated a term for substrate inhibition. Multiple determinations of initial rates at a specific set of component concentrations provided measures of assay precision, and weighted mean data were used.

**Determination of Protein Concentration.** The concentrations of the wild-type and the Arg-22 → Ala enzymes were determined using the Lowry method (Lowry et al., 1951) with bovine serum albumin as the standard.

**Other Methods.** SDS–polyacrylamide gel electrophoresis was used to judge enzyme homogeneity (Laemmli, 1970). Concentrations of Fru-1,6-*P*<sub>2</sub> and NADP were checked by performance in the coupled assay, of AMP using 15.4 as the millimolar extinction coefficient at pH 7.0 at 259 nm, and of Fru-2,6-*P*<sub>2</sub> by partial acid hydrolysis and analysis of fructose 6-phosphate (Pilkis et al., 1981).

## RESULTS

**Kinetic Properties of the Arg-22 → Ala Fru-1,6-*P*<sub>2</sub>ase.** After purification to homogeneity, the Arg-22 → Ala Fru-1,6-*P*<sub>2</sub>ase exhibited a slightly lower *K*<sub>m</sub>, a slightly higher *V*<sub>max</sub>, and an enhanced level of substrate inhibition compared to the wild-type enzyme (Figure 2). Due to the enhanced substrate inhibition observed for the mutant enzyme, analysis of the kinetic data was performed using a nonlinear least-squares method incorporating a term for substrate inhibition. Since the wild-type enzyme also exhibits substrate inhibition, although at lower levels, analysis of the kinetic data for the wild-type enzyme was performed in an identical fashion. The *V*<sub>max</sub> of the Arg-22 → Ala enzyme, 44 µmol·min<sup>−1</sup>·mg<sup>−1</sup>, was elevated about 30% compared to the value observed for the wild-type enzyme, 34 µmol·min<sup>−1</sup>·mg<sup>−1</sup>. The catalytic efficiency of the Arg-22 → Ala enzyme increased, compared to the wild-type enzyme, not only because of an increase in the *k*<sub>cat</sub> but also because of a slight decrease in the *K*<sub>m</sub>, from 1.4 µM observed for the wild-type to 1.1 µM observed for the Arg-22 → Ala enzyme (Table 1). Analysis of the substrate saturation curves indicated that there was a substantial enhancement in the ability of the substrate to inhibit the Arg-22 → Ala compared to the wild-type enzyme.

**Influence of Mg<sup>2+</sup> on the Wild-Type and Mutant Enzymes.** Wild-type Fru-1,6-*P*<sub>2</sub>ase is activated by Mg<sup>2+</sup>, and this

Table 1: Kinetic Parameters for Wild-Type and Arg-22 → Ala Fru-1,6- $P_2$ ases<sup>d</sup>

enzyme	$k_{cat}$ (s <sup>-1</sup> )	$K_m$ (Fru-1,6- $P_2$ ) (μM)	[Mg <sup>2+</sup> ] <sub>0.5</sub> <sup>a</sup> (mM)	$K_{0.5}$ (AMP) <sup>b</sup> (μM)	$K_i$ (Fru-2,6- $P_2$ ) (μM)
wild-type	21 ± 1	1.4 ± 0.3	0.34	4.4 <sup>c</sup>	0.065 ± 0.005
Arg-22 → Ala	27 ± 1	1.1 ± 0.1	0.27	44 <sup>c</sup>	0.029 ± 0.002

<sup>a</sup> The concentration of Mg<sup>2+</sup> required to activate the enzyme half of the maximal extent. <sup>b</sup> The concentration of AMP required to inhibit the enzyme by 50%. <sup>c</sup> 3 mM Mg<sup>2+</sup>. <sup>d</sup> Experiments on the wild-type and the Arg-22 → Ala enzyme were performed at 17.5 μM Fru-1,6- $P_2$  and 2 mM magnesium concentrations when the components were held constant, except as noted.

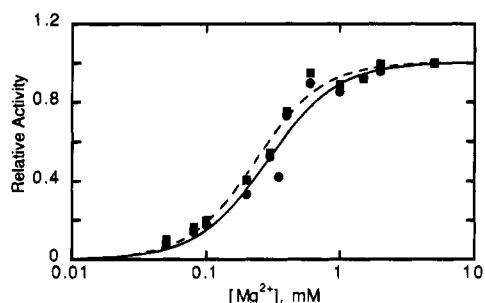


FIGURE 3: Influence of Mg<sup>2+</sup> on the activity of the wild-type (●, solid line) and the Arg-22 → Ala (■, dashed line) Fru-1,6- $P_2$ ases at 17.5 μM Fru-1,6- $P_2$ . Assays were performed under the same conditions as mentioned in the legend to Figure 2. Because of the differences in specific activity between the wild-type and mutant enzymes, the rates were normalized to the values obtained at saturating Mg<sup>2+</sup> (5 mM).

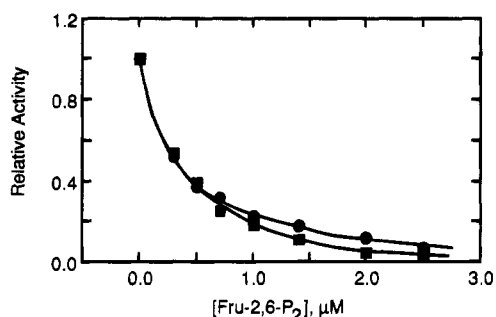


FIGURE 4: Inhibition by Fru-2,6- $P_2$  of the wild-type (●) and the Arg-22 → Ala (■) Fru-1,6- $P_2$ ases, expressed as activity relative to inhibitor-free rates, at 2 mM Mg<sup>2+</sup> and 7 μM Fru-1,6- $P_2$ . Assays were performed under the same conditions as described in the legend to Figure 2.

activation is cooperative with a Hill coefficient of approximately 2 (Nimmo & Tipton, 1975b). As seen in Figure 3, Mg<sup>2+</sup> activated both the wild-type and the Arg-22 → Ala enzymes to almost identical extents. However, these data suggest that the affinity of the Arg-22 → Ala enzyme for Mg<sup>2+</sup> was slightly higher than that of the wild-type enzyme. The concentration of Mg<sup>2+</sup> required to activate the wild-type enzyme to half of its maximal activity was 0.34 mM compared to 0.27 mM for the Arg-22 → Ala enzyme.

**Influence of Fru-2,6- $P_2$  on the Wild-Type and Mutant Enzymes.** Wild-type Fru-1,6- $P_2$ ase is inhibited by Fru-2,6- $P_2$ , and this inhibition is competitive with the substrate Fru-1,6- $P_2$ . As seen in Figure 4, Fru-2,6- $P_2$  inhibited the wild-type and Arg-22 → Ala enzymes in an almost identical fashion. The  $K_i$  for Fru-2,6- $P_2$  of the Arg-22 → Ala enzyme was less than half that of the wild-type enzyme (Table 1).

**Influence of AMP on the Wild-Type and Mutant Enzymes.** Just as observed with the wild-type enzyme, the Arg-22 → Ala enzyme could be completely inhibited by AMP. However, AMP inhibition of the mutant enzyme was substantially different than that found for the wild-type enzyme. As illustrated in Figure 5, the Arg-22 → Ala enzyme required

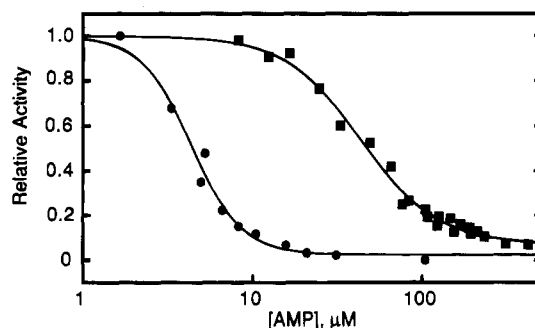


FIGURE 5: Inhibition by AMP of the wild-type (●) and the Arg-22 → Ala (■) Fru-1,6- $P_2$ ases, expressed as activity relative to inhibitor-free rates, at 3 mM Mg<sup>2+</sup> and 17.5 μM Fru-1,6- $P_2$ . Assays were performed under the same conditions as described in the legend to Figure 2.

more than 10-fold higher concentrations of AMP to be inhibited to the same extent. The concentration of AMP required to inhibit the wild-type enzyme to half of its maximal activity was 4.4 μM compared to 44 μM for the Arg-22 → Ala enzyme (Table 1).

## DISCUSSION

A comparison of the X-ray crystallographic structures of the R and T states of pig kidney Fru-1,6- $P_2$ ase indicates a major change in the quaternary structure of the enzyme upon the binding of the allosteric inhibitor AMP (Ke et al., 1991a). This change in quaternary structure involves a rotation of the lower dimer C3:C4 relative to the upper dimer C1:C2 by 17°. In both the R and T states, the interfaces between the upper and lower dimers are stabilized by specific sets of interactions between amino acid residues of different subunits. The rotation of the two dimers during the R → T transition breaks one set of interactions that stabilize the R state and allows the formation of a different set of interactions that stabilize the T state of the enzyme. Although the structural data suggest that these intersubunit interactions are important for stabilization of the R and or T states, these data do not provide direct information concerning the functional role of these residues in the R → T transition.

Here we report studies related to the function of Arg-22, which is involved in different intersubunit interactions in the R and T states of the enzyme. When Arg-22 in pig kidney Fru-1,6- $P_2$ ase was replaced by alanine, there was not only an increase in the  $V_{max}$  of the enzyme-catalyzed reaction, but also a slight decrease in the  $K_m$ , resulting in an enzyme with a 65% enhancement of catalytic efficiency as judged by the  $k_{cat}/K_m$  ratio. The higher affinity for Fru-1,6- $P_2$  observed in the Arg-22 → Ala enzyme also was reflected in the more than 2-fold enhanced affinity of the mutant enzyme for the competitive inhibitor Fru-2,6- $P_2$ , as well as an enhancement in substrate inhibition. All these factors suggest that the Arg-22 → Ala enzyme in the absence of AMP has a destabilized T allosteric state, and can be described as an

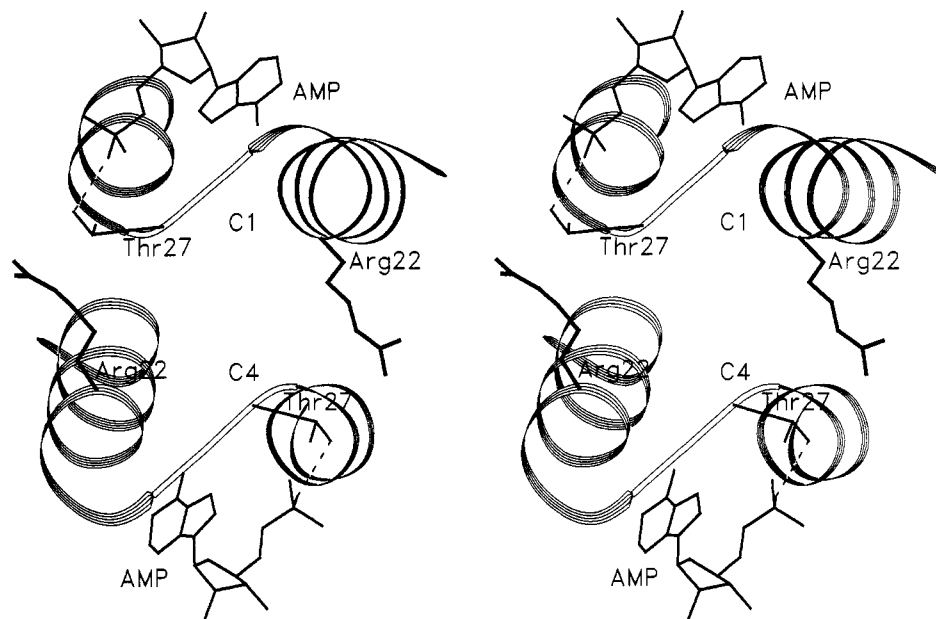


FIGURE 6: Stereoview of the C1:C4 interface of pig kidney Fru-1,6- $P_2$ ase in the T state (Ke et al., 1991a). Shown are portions of helices H1 and H2 that flank the AMP binding site. The side-chain hydroxyl of Thr-27 interacts with a phosphate oxygen of AMP, while the backbone carbonyl oxygen of Thr-27 forms a hydrogen bond with the side chain of Arg-22. This figure was drawn with the program SETOR (Evans, 1993).

R-state enzyme possessing enhanced catalytic potential. The enhanced catalytic efficiency as well as the ability of the mutant enzyme to be activated by  $Mg^{2+}$  also indicates that the replacement of Arg-22 by Ala has in no way diminished the ability of the enzyme to catalyze the hydrolysis of Fru-1,6- $P_2$ .

The major kinetic alteration caused by the substitution of Arg-22 by Ala was the decreased affinity of the enzyme for the allosteric effector AMP, demonstrated by the 10-fold increase in the concentration of AMP required to inhibit the enzyme. Although this alteration must be due to a weakening of the interactions between the enzyme and the inhibitor, the cause of this affinity loss may be direct or indirect. In the R state, the side chain of Arg-22 is more than 8 Å from Thr-27, the residue with which it interacts in the T state. Therefore, a replacement at Arg-22 might not be expected to have a direct influence on AMP binding to the R state of the enzyme. However, the R  $\rightarrow$  T transition results in a substantial alteration in the interactions involving this residue that span both the C1:C4 and C2:C3 interfaces. In the T state, the guanidino group of Arg-22 is within hydrogen bonding distance to the carbonyl oxygen of Thr-27. Although the carbonyl oxygen of Thr-27 does not interact with AMP, the side chain hydroxyl of this Thr-27 does interact with a phosphate oxygen of AMP (Ke et al., 1991a). Therefore, in the T state, it is possible that the replacement of Arg-22 by Ala may have a direct influence on the binding of AMP by disturbing the protein backbone near Thr-27. However, the loss of AMP affinity due to a protein backbone displacement is unlikely because helices H1 and H2 stabilize the conformation of the turn containing residue Thr-27 between them (see Figure 6).

The enhanced affinity of the Arg-22  $\rightarrow$  Ala enzyme for Fru-1,6- $P_2$  and Fru-2,6- $P_2$  as well as the higher  $k_{cat}$  value suggests an enzyme in which the equilibrium between R and T is shifted more toward the R state than is characteristic of the wild-type enzyme. Given this hypothesis, the altered affinity for AMP would be reflected in the weakened

stabilization of the T state due to the loss of the interactions of Arg-22 across the C1:C4 and C2:C3 interfaces. Such a destabilization of the T state can explain all the observed alterations in the kinetic properties of the Arg-22  $\rightarrow$  Ala enzyme.

As pointed out by Ke et al. (1991a), arginine is uniformly present at residue 22 in the Fru-1,6- $P_2$ ases that are inhibited by AMP, but absent in certain Fru-1,6- $P_2$ ases that are not inhibited by AMP. The data reported here suggest that a substitution at Arg-22 may be partially but not totally responsible for the loss of AMP inhibition observed in these enzymes.

The X-ray structural data indicate that the T-state intersubunit interaction between Arg-22 and the backbone carbonyl of Thr-27 is only one of several interactions that stabilize the C1:C4 and C2:C3 interfaces. Furthermore, many of these intersubunit interactions are different in the R and T states of the enzyme. Therefore, the interactions involving Arg-22 contribute only a part to the overall stabilization of T allosteric state over the R allosteric state. Additional experiments are planned to further evaluate the functional role of the remaining intersubunit interactions in the R  $\rightarrow$  T transition of pig kidney Fru-1,6- $P_2$ ase.

## REFERENCES

- El-Maghrabi, M. R., & Pilakis, S. J. (1991) *Biochem. Biophys. Res. Commun.* 176, 137–144.
- Evans, S. V. (1993) *J. Mol. Graphics* 11, 134–138.
- Giroux, E., Williams, M. K., & Kantrowitz, E. R. (1994) *J. Biol. Chem.* 269, 31404–31409.
- Ke, H. M., Thorpe, C. M., Seaton, B. A., Lipscomb, W. N., & Marcus, F. (1989a) *J. Mol. Biol.* 212, 513–539, and correction (1990) *J. Mol. Biol.* 214, 950.
- Ke, H. M., Thorpe, C. M., Seaton, B. A., Marcus, F., & Lipscomb, W. N. (1989b) *Proc. Natl. Acad. Sci. U.S.A.* 86, 1475–1479.
- Ke, H. M., Zhang, Y., & Lipscomb, W. N. (1990) *Proc. Natl. Acad. Sci. U.S.A.* 87, 5243–5247.
- Ke, H. M., Liang, J.-Y., Zhang, Y., & Lipscomb, W. N. (1991a) *Biochemistry* 30, 4412–4420.

- Ke, H. M., Zhang, Y., Liang, J.-Y., & Lipscomb, W. N. (1991b) *Proc. Natl. Acad. Sci. U.S.A.* 88, 2989–2993.
- Kunkel, T. A. (1985) *Proc. Natl. Acad. Sci. U.S.A.* 82, 488–492.
- Kunkel, T. A., Roberts, J. D., & Zakour, R. A. (1987) *Methods Enzymol.* 154, 367–382.
- Laemmli, U. K. (1970) *Nature (London)* 227, 680–685.
- Liang, J.-Y., Zhang, Y., Huang, S., Ke, H., & Lipscomb, W. N. (1992) *Proc. Robert A. Welch Found. Conf. Chem. Res.*, 36th, 57–99.
- Lowry, O. H., Rosebrough, N. J., Farr, A. L., & Randell, R. H. (1951) *J. Biol. Chem.* 193, 265–275.
- Marcus, F., Edelstein, I., Reardon, I., & Heinrikson, R. L. (1982) *Proc. Natl. Acad. Sci. U.S.A.* 79, 7161–7165.
- Nimmo, H. G., & Tipton, K. F. (1975a) *Eur. J. Biochem.* 58, 575–585.
- Nimmo, H. G., & Tipton, K. F. (1975b) *Eur. J. Biochem.* 58, 567–574.
- Pilkis, S. J., & Claus, T. H. (1991) *Annu. Rev. Nutr.* 11, 465–515.
- Pilkis, S. J., El-Maghrabi, M. R., Pilkis, J., & Claus, T. (1981) *J. Biol. Chem.* 256, 3619–3622.
- Riou, J.-P., Claus, T. H., Flockhart, D. A., Corbin, J. D., & Pilkis, S. J. (1977) *Proc. Natl. Acad. Sci. U.S.A.* 74, 4615–4619.
- Sanger, F., Nicklen, S., & Coulson, A. R. (1977) *Proc. Natl. Acad. Sci. U.S.A.* 74, 5463–5467.
- Sedivy, J. M., Daldal, F., & Fraenkel, D. G. (1984) *J. Bacteriol.* 158, 1048–1053.
- Taketa, K., & Pogell, B. M. (1965) *J. Biol. Chem.* 240, 651–662.
- Vieira, J., & Messing, J. (1987) *Methods Enzymol.* 153, 3–11.
- Williams, M. K., & Kantrowitz, E. R. (1992) *Proc. Natl. Acad. Sci. U.S.A.* 89, 3080–3082.
- Zhang, Y., Liang, J.-Y., Huang, S., & Lipscomb, W. N. (1994) *J. Mol. Biol.* 244, 609–624.

BI951407X